DEPENDENCE OF THE BEAGLE2 TRAJECTORY ON THE MARS ATMOSPHERE

Rainer Bauske

TERMA GmbH, ESOC Darmstadt, OPS-GFI
Robert-Bosch-Str. 5, D-64293 Darmstadt, Germany
Phone: +49 (0)6151 902795, Fax: +49 (0)6151 902271
Email: Rainer.Bauske@esa.int

ABSTRACT

Six days before arrival, the Mars Express spacecraft released the landing probe Beagle2. This paper extends a reconstruction of the lander's drift trajectory from atmospheric entry to landing. Uncertainties of the initial drift trajectory and contributions by uncertainties in the atmospheric descent computation are mapped to the landing site. Parameters of key events during the descent are derived and compared to nominal target values. Special attention is paid to the dependence of the trajectory computation on the choice of the atmosphere model. Although different atmosphere models lead to differences in the computed trajectories, the final deviations of the landing points are small compared to the uncertainty by the initial state vector before ejection.

1. BACKGROUND

The Mars lander Beagle2 has been ejected on December 19th, 2003, from the Mars Express spacecraft (s/c), six days prior to its arrival. Unfortunately, the contact to Beagle2 after landing could never be established. The ejection was performed using a spring release mechanism causing a Δv along the spacecraft +z axis and a rotational movement of the lander. From the ejection onward, the lander's journey to Mars was completely passive because it had no attitude or orbit control system. Its attitude was maintained by spinning with about 14 revolutions per minute.

At ejection the lander therefore had to be targeted:

- To achieve at the atmospheric entry point a nominal angle between the lander trajectory and a horizontal atmospheric layer of -16.5 deg, referred to as entry angle. The corridor of allowed entry angles is 2 deg wide (with +1 deg = +3σ, -1 deg = -3σ). The atmospheric entry point is defined at where the lander reaches 120 km height normal to the surface of the reference ellipsoid.
- To arrive at a height where the drag acceleration becomes important with its major axis aligned with the direction of its velocity relative to the atmosphere (aerodynamic velocity). This is referred to as the height of zero angle of attack, defined at 100.5 km height above the reference ellipsoid. The allowed 3σ error is 3 deg.

- To reach the nominal planned landing site, specified with respect to the reference ellipsoid with 11.6 deg areocentric northward latitude, 90.74 deg eastward longitude, at –3367 m height normal to the reference ellipsoid (areocentric system in [2])

The lander trajectory is split into the free drift motion of the lander from release until atmospheric entry and into the part from atmospheric entry onwards.

Relevant parameters and models for the drift trajectory computation such as the initial state vector, the release Delta-V vector, and the solar radiation pressure model are explained in detail in the accompanying paper of R. Cramm et al., [1], which focuses on the drift part and on the error propagation of initial uncertainties.

This paper concentrates on the atmospheric part and shows how it depends on the range of entry-conditions compatible with our best knowledge of the Beagle2 release from Mars Express, as reconstructed in [1]. The influence of the atmosphere is illustrated by comparison of the reconstructed trajectory with results from using a range of different atmosphere models.

Starting at entry into the atmosphere of Mars the descent trajectory can be split into various phases: In the first part with supersonic speed the deceleration and heating by the atmosphere increase to maximum values and decrease thereafter. During this phase the probe is protected by an aeroshell, which consists of front shield and back cover. After drogue chute opening, the speed decreases from supersonic to subsonic values. After transonic deceleration front shield and back cover are released simultaneously, where the drogue chute removes the back cover. The main chute inflation separates the lander from the front shield and leads to a nearly vertical descent. At around 280 m height above ground the inflation of the airbags starts and initiates the landing.

The atmosphere model enters the trajectory computation via the atmospheric drag force acting on the vehicle. Direct atmosphere dependent parameters of the force are the density and the speed of the vehicle relative to the wind. The drag coefficient depends on parameters of the vehicle as well as on Mach number, Knudsen number, and Reynolds number where the latter depend on density and temperature as well as on the atmospheric composition and parameters specific for each gas species.

ESOC and the Beagle2 Lander Consortium derived physical models to compute the atmospheric descent and agreed on a final set specified in the Interface Control Document (ICD) [2]. This set provides the background for the computations in this paper, which start at ejection and stop at the beginning of the airbag inflation, neglecting the horizontal drift on the final small part of the trajectory.

In the following the angle of attack error ellipse and the landing error ellipse are presented as functions of the various error sources. Peak deceleration, time and height of the drogue chute opening and the landing site and speed are shown for available atmosphere models with and without inclusion of effects by wind.

For this purpose the lander descent is modelled with 3 degree of freedom using the ESOC operational manoeuvre optimisation software MANTRA, which incorporates the physical models and the descent timeline agreed between ESOC and the Beagle2 Lander Consortium.

2. DESCENT TIMELINE

Within MANTRA the descent timeline consists of the following events:

Entry: Defined at altitude 120 km above the reference ellipsoid.

Zero angle of attack height: At altitude 100.5 km above the reference ellipsoid, the angle of attack should be zero degrees, which means that the lander attitude is aligned with the aerodynamic velocity.

Loss of multi layer insulation (MLI): The MLI layer (0.4 kg) is lost between 90 to 80 km height because of aerodynamic heating and shear.

Drogue chute opening command: The command is issued at reaching deceleration of –0.77 g, where g is defined as 9.81 m/s^2.

Drogue chute opening: Drogue chute drag is switched on with a delay of 0.1 s after the drogue chute opening command to account for any hardware delay, deployment period, and inflation time etc.

Separation of drogue chute and back cover: Drogue chute and back cover are separated 44.0 s after the drogue chute opening command.

Front shield separation: Lander mass and reference area are reduced immediately at drogue chute and back cover separation.

Main chute opening: Main chute drag is enabled after a deployment period of $T_{dep} = 3.67 - 0.0159\, V_{bc}$ seconds after the drogue chute separation, where V_{bc} is the lander velocity at back cover release in (m/s).

The main chute is fully inflated after a further $T_{inf} = k/V_S$ seconds. During this period (the inflation time) the parachute drag coefficient is modelled as a function of time and velocity taken at the start of inflation. V_S is the lander speed at the end of deployment in (m/s), i.e. at back cover release time plus T_{dep}, and k_f has a value of 80.0 m.

The variation of drag coefficient with time is given by $CD/CD_0 = 0.008 + 0.992\, (t/T_{inf})^{1/2}$, where t is the time from the end of deployment (start of inflation) and CD_0 is the drag coefficient for full inflation.

Landing: Landing is specified by altitude above the reference ellipsoid. Here it is set to the radar trigger altitude 280 m above terrain. The radar trigger altitude is equivalent to a height of 3087 m below the reference ellipsoid, measured normal to the surface.

3. ATMOSPHERE MODELS

The atmosphere models are engineering – oriented models, which provide density, pressure, temperature, and velocity of the wind. It should be noted that these models basically simulate a 'mean' atmosphere for the time and location of the descent while real conditions might be severe.

Mars-GRAM 38 is based on ad-hoc parameterisations to data observed by Mariner and Viking missions [3].

Mars-GRAM 2000 and Mars-GRAM 2001 are based on data tables of output from the NASA AMES Mars General Circulation Model (MGCM) and the University of Arizona Mars Thermospheric General Circulation Model (MTGCM). The GCM models are based on first-principles physics, e.g. atmospheric thermodynamics and equations of atmospheric motions. They have been tuned to represent the Mariner and Viking results at times and locations for which these data are available. Mars-GRAM 2000 contains a density wave model based on Mars Global Surveyor (MGS) accelerometer data [4]. Mars-GRAM 2001 internally uses high-resolution topographic data obtained with the MOLA instrument of MGS. The resolution is here 0.5 deg instead of 7 by 9 deg as in the earlier models [5].

The Mars Climate Database 3.0 (MCD) is a database of atmospheric statistics compiled from simulations of General Circulation Models developed at Laboratoire de Météorologie Dynamique du CNRS, France and the University Oxford, United Kingdom. For details on the Database refer to [6]. For details on the GCM models and the simulations refer to [7] and [8].

The atmosphere model 'ICD' was used operationally. It had been provided by the Beagle2 Lander Consortium and consists of a table of the atmospheric parameters density, temperature, pressure, and velocity components of wind as function of height [2]. The table is based on output of the European Mars Climate Database (EMCD), version 3.1 (or newer) by the Oxford University Department of Atmospheric Physics and represents the 'best guess' for the entry to the chosen landing site and time. The data are relative to the local terrain height at the landing site (although the profile is taken at the maximum deceleration position), and have been corrected relative to the MOLA/Goddard Reference Ellipse. A logarithmic interpolation on pressure and density is performed, while a linear interpolation is used for temperature.

4.   REFERENCE ELLIPSOID

The atmospheric entry height, the zero angle of attack height and the landing site are defined w.r.t. the reference ellipsoid given by:

Equatorial radius $r_{equator} = 3396.0$ km

Flatness $f = 1 - \dfrac{r_{pol}}{r_{equator}} = 0.005206125$

5.   UNCERTAINTIES CONSIDERED IN THE TRAJECTORY RECONSTRUCTION

This chapter summarizes data from the trajectory reconstruction in paper [1] and adds uncertainties assumed for the atmospheric descent. The computation of errors proceeds as outlined in [1], but taking into account all uncertainties named in this chapter. We concentrate on the angle of attack errors and the landing ellipse.

5.1   Initial spacecraft state

From a dedicated orbit determination the 1σ position uncertainty of Mars Express at ejection is < 3 km and the velocity uncertainty is < 9 mm/s.

5.2   Ejection Δv magnitude and direction

The ejection took place at 2003/12/19 08:32:14.184 barycentric dynamical time (TDB) (central time). Its expected duration [2] was 0.117 s and the expected Δv for the lander (based on equations in [2]) was 0.2919 m/s. From the available data Cramm et al. [1] deduce an over-performance of the Δv magnitude of (1.3 ± 0.5) % (1σ) resulting in a Δv of 0.2957 m/s. The lander is ejected in +z direction of Mars Express, which means that the spacecraft had to be on a collision trajectory

with Mars. The 1σ direction error of the spin up and ejection mechanism (SUEM) is 0.14° [2], which translates to errors of 0.14° in declination and 0.155° in right ascension of the mean ecliptic system of 2000. The s/c attitude error at ejection can be conservatively estimated to be < 10 % of the SUEM error. In the computations below it is therefore neglected. The initial mass of the lander is 68.86 kg, assumed to be exact.

5.3   Solar radiation pressure

Solar radiation impacts the lander from behind throughout its trajectory with a solar aspect angle of ~124°. The lander's shape is approximated by bottom and mantle of a truncated cone with geometry derived from [2]. Projecting the parts of this shape visible from the sun onto a plane normal to the incident radiation results in an area of 0.39755 m^2 of a flat plate radiation pressure model. The absorptivity coefficient of 0.14 (see [1]) and the assumption, that 50% of the reflection is specular while the other 50 % is diffusive, leads to a solar radiation pressure coefficient of 1.33444 for Beagle2. The 1σ uncertainty is taken to be 25 % as there is low confidence on the optical properties of Beagle2.

5.4   Drag coefficients

The 1σ uncertainty of each of the used drag coefficient models is assumed as 5 %.

5.5   Threshold acceleration for drogue chute opening

The drogue chute opening initiates the change in the trajectory from a nearly horizontal to a vertical direction. Many comparisons between computations using different atmosphere models as well as cross comparisons between entire different trajectory computation programs (MANTRA w.r.t. reference program used by Beagle2 consortium and w.r.t. program used by ESA Mission Analysis) showed that the time and height of the drogue chute opening are the most important parameters to achieve agreement between landing points resulting from different computations. Time and height of the opening are directly controlled via the threshold acceleration value. Here we assume that the accelerometer on board has a 1σ uncertainty of 3 %.

5.6   Atmospheric wind

Wind magnitude and direction are not known very well and therefore winds are neglected in computations of the nominal trajectory. The values of the velocity computed with the ICD atmosphere model in eastward and northward direction are taken as 1σ errors.

6. RESULTS

6.1 Reconstructed trajectory

First we present results for the reconstructed trajectory where all computations use the nominal atmosphere model ICD.

Fig. 1 shows the tilt of the lander attitude (assumed equal to ejection direction because conservation of lander spin) w.r.t. the aerodynamic velocity direction at the angle of attack height 100.5 km, and 3σ error ellipses corresponding to the various uncertainties. The error ellipses are 'accumulated' which means that more and more uncertainties are added to the base line computation. Semi major and semi minor axes are given Table 1.

Uncertainties due to the drag coefficients of the aeroshell and the solar radiation pressure (s.r.p.) coefficient are small compared to the uncertainty of the ejection. A notable contribution arises from the wind field. For operations it was required that the 3σ error should be smaller than $3°$.
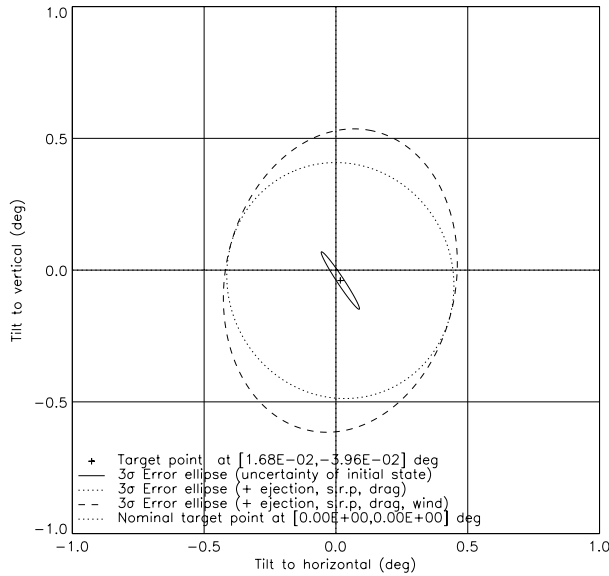
Fig. 1. Tilt of lander attitude w.r.t. relative velocity

Fig. 2 shows the reconstructed and the nominal landing points. Again the plot shows accumulated error ellipses for the various uncertainties. The basic error ellipse is determined by the initial state uncertainty. Other uncertainties seem to increase its width more than its length. This effect results from the orientation of the initial ellipse w.r.t. the equator. Any delay or shortening of the descent time will lead to a different longitude of the landing point and cause a widening and rotation of the ellipse. Semi major and semi minor axes of the landing error ellipse are given in Table 2.

Table 1. Axes of angle of attack error ellipse

Additive Uncertainty	Semi major axis (deg)	Angle to horiz. axis (deg)	Semi minor axis (deg)
initial state	0.130	-56.56	0.013
+ ejection + s. r. p. + drag	0.452	-66.69	0.427
+ wind	0.581	78.12	0.437
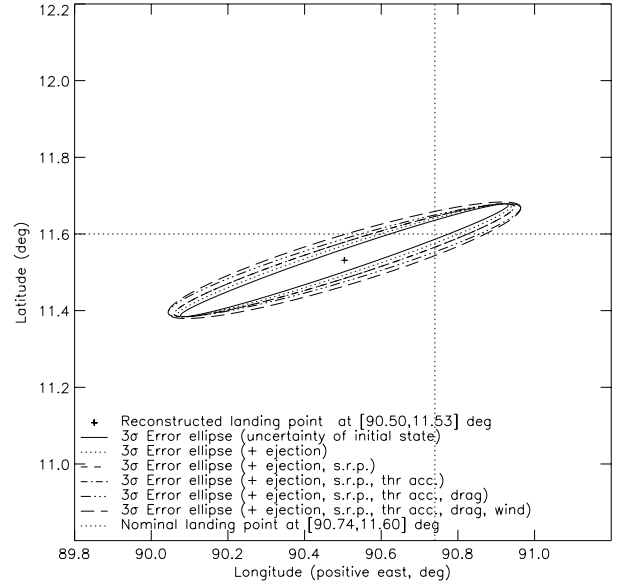
Fig. 2 Reconstructed landing point and error ellipse

Table 2. Axes of landing error ellipses

Additive Uncertainty	Semi major axis (km)	Angle to latitude axis (deg)	Semi minor axis (km)
initial state	26.8	18.69	1.8
+ ejection	27.2	18.19	2.2
+ s. r. p.	27.6	17.64	2.7
+ thr. acc.	27.6	17.63	2.7
+ drag	28.4	16.75	3.2
+ wind	28.5	16.81	3.8

6.2 Effects of atmosphere model choice

6.2.1 Density and temperature along trajectory

The differences of the atmosphere models can be seen by comparison of their densities and temperatures along the reconstructed nominal trajectory as function of height w.r.t. the reference ellipsoid in Fig. 3 and 4, respectively. As to be expected, the ICD and MCD model values are close together. These models predict higher densities in the upper part of the atmosphere than the new (2000/2001) Mars-GRAM models. The temperatures diverge and show opposite trends above

110 km height. Speed of sound and Mach number (not plotted) strongly depend on temperature and therefore show similar relative deviations.
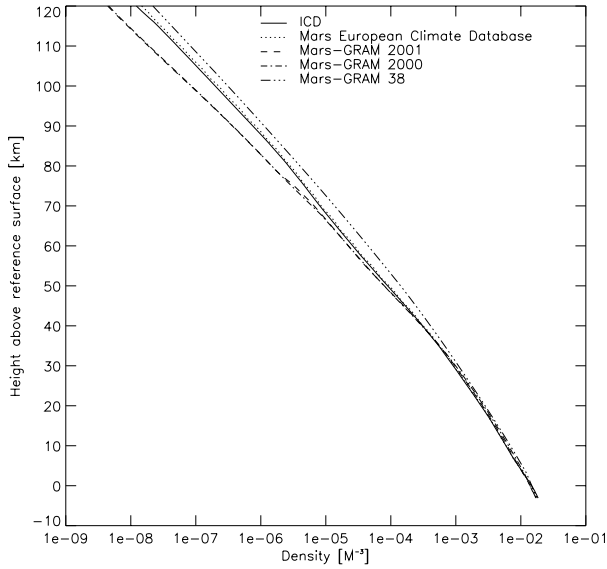
Fig. 3. Density along reconstructed trajectory
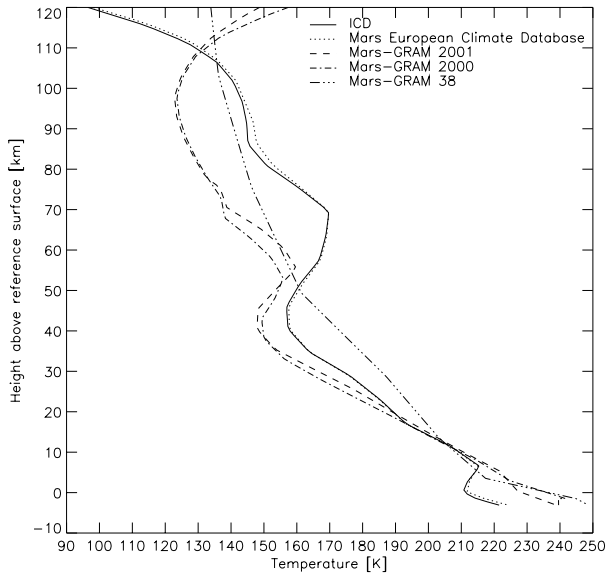
Fig. 4. Temperature along reconstructed trajectory

6.2.2 Trajectory dependence on atmosphere model

Computing now trajectories with each one of the atmosphere models with and without winds we arrive at the following results:

Peak deceleration, Fig. 5: Peak deceleration occurs between 24 and 26 km height above the reference ellipsoid with values between 125 to 140 m/s^2. All Mars-GRAM models show higher decelerations above the peak and lower ones below the peak than the ICD / MCD models, where Mars-Gram 2001 agrees best.
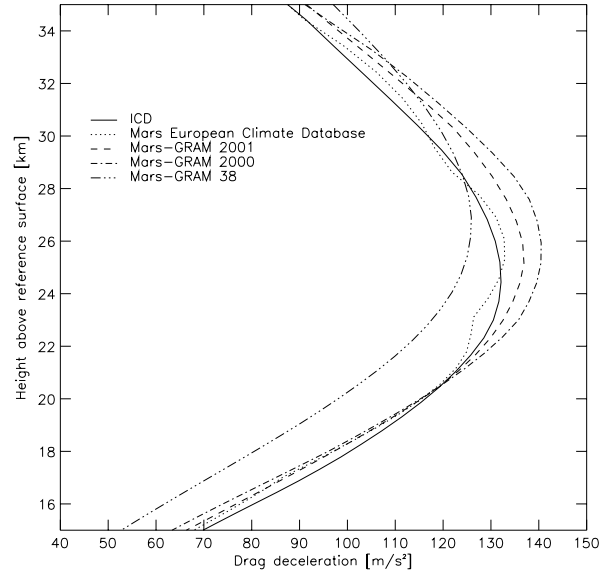
Fig. 5. Peak deceleration

Times and heights of drogue chute opening command, Table 3.: The Mars-GRAM models shorten the time from entry to the drogue chute opening command compared to the ICD/MCD models, which is a consequence of the smaller values of the drag below the peak deceleration region. The effect of wind is small for the ICD/MCD models, while it amounts to ~1 km height difference for the newer Mars-GRAM models.

Table 3. Time and altitude of drogue chute opening command

	Time	ΔTime	Height	ΔHeight
Without wind	[s]	[s]	[km]	[km]
Reconstructed	144.63	0.00	3.35	0.00
MCD	144.65	0.02	3.46	0.11
Mars-GRAM 2001	142.74	-1.89	3.99	0.64
Mars-GRAM 2000	141.67	-2.96	4.51	1.16
Mars-GRAM 38	142.68	-1.95	5.19	1.84
With wind				
ICD	145.41	0.78	3.23	-0.12
MCD	145.55	0.92	3.32	-0.03
Mars-GRAM 2001	142.76	-1.87	3.96	0.61
Mars-GRAM 2000	141.76	-2.87	4.48	1.13
Mars-GRAM 38	143.63	-1.00	4.98	1.63

Times and heights of main chute inflation start: The trends seen in Table 3 are continued by all models as a consequence of the short interval between drogue and main chute opening. Mars-GRAM 2001 agrees to 2 s (about 500 m) with the ICD / MCD model solutions. Times range from 187.9 to 191.9 s wrt. time of entry, heights from –1.06 to +0.79 km wrt. reference ellipsoid.

Landing point location, Fig. 6 without, Fig. 7 with wind: Solutions using ICD and MCD are close together, while Mars-GRAM 2001 agrees best. All landing points tend to be on similar latitudes, owing to the small

inclination of the Beagle2 orbit plane wrt. the Mars equator at entry. The difference between landing points obtained with Mars-GRAM 2001 and those obtained with the ICD/MCD models are about 2.1 km (with wind), which is small compared to the semi major axis of the landing error ellipse (28.5 km). Winds drive the lander towards southeast, but again their effect appears to be small compared to the dimension of the landing error ellipse. Results from Mars-GRAM 38 are very different from the other models as they have been in all comparisons above.
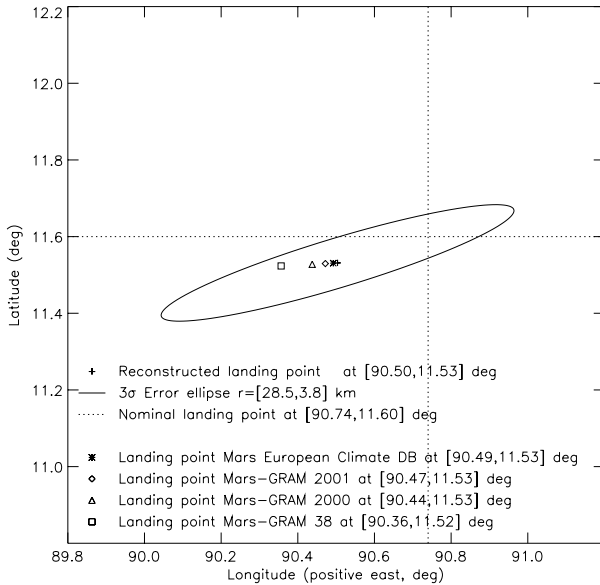
Fig. 6. Landing points computed without wind

Landing speed, Table 4. The average downward landing velocity is 16.1 m/s. Winds contribute between 6.5 and 11.6 m/s in horizontal direction according to the newer atmosphere models.
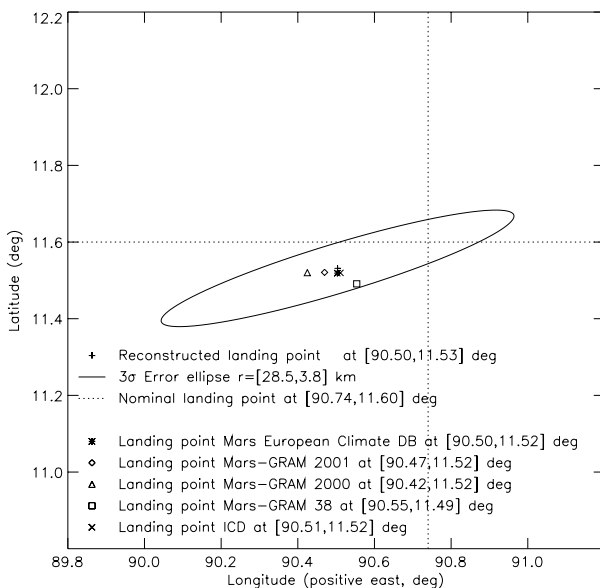
Fig. 7. Landing points computed with wind

Table 4. Landing speed

With wind	Vertical [m/s]	Horizontal [m/s]
ICD	-15.80	6.46
MCD	-16.07	9.12
Mars-GRAM 2001	-16.45	11.57
Mars-GRAM 2000	-16.29	4.24
Mars-GRAM 38	-16.06	2.84

7. SUMMARY

The Beagle2 trajectory has been reconstructed starting from the observed spacecraft state at ejection. Estimated uncertainties have been mapped through to start of airbag inflation (280m above ground), resulting in a landing ellipse with semi axes of [28.5, 3.8] km and centre at 90.50° east, 11.53° north and –3087 m height w.r.t. the reference ellipsoid (areocentric coordinate system specified in [2]). The centre is in 14.3 km distance to the nominal landing point. The angle between major axis and latitude axis is 16.81°. The initial state vector contributes the main uncertainty for the landing location. Differences arising from the choice of atmosphere model tend to become smaller for newer models. However, temperatures and densities of the Mars-GRAM (38/2000/2001) models disagree with those in the European Climate Database (V3.0-V3.1) and for fine-tuning of future missions both strains of models should be considered.

REFERENCES

1.   Cramm R. C., et al., Reconstructed Beagle2 Trajectory, ISFFD 2004.

2.   Smith A. and Clemmet J., MEX Lander Delivery Module: Beagle2 - Esoc Interface, Astrium, BEA2.ICD.00005.S.MMS.

3.   Justus C. G. and B. F. James, Mars Global Reference Atmosphere Model (Mars-GRAM) Version 3.8: User Guide, NASA/TM-1999-209629, 1999.

4.   Justus C. G. and B. F. James, Mars Global Reference Atmosphere Model 2000 Version (Mars-GRAM 2000): Users Guide, NASA/TM-2000-210279, 2000.

5.   Justus C. G. and B. F. James, Mars Global Reference Atmosphere Model 2001 Version (Mars-GRAM 2001): Users Guide, NASA/TM-2001-210061, 2000.

6.   Lewis S. R., et al., Mars Climate Database V3.0 - User Manual, ESTEC Contract 11369/95/NL/JG, 2001.

7.   Lewis, S. R., et al., A Climate Database for Mars, J. Geophys. Res., vol. 104, p. 24177-24194, 1999.

8.   Forget F., et al., Improved general circulation models of the martian atmosphere from the surface to above 80 km, J. Geophys. Res., vol. 104, p. 24155-24176, 1999.

9.   Smith D. E., et al., An Improved Gravity Model for Mars: Godard Mars Model 1, J. Geophys. Res., vol. 98, no. E11, p. 20871-20889, 1993.